The Distribution of Tropical Thin Cirrus Clouds Inferred from *Terra* MODIS Data

A. E. DESSLER

Earth System Science Interdisciplinary Center, University of Maryland at College Park, College Park, Maryland

P. YANG

Department of Atmospheric Sciences, Texas A&M University, College Station, Texas

(Manuscript received 15 May 2002, in final form 4 September 2002)

ABSTRACT

Thin cirrus clouds (with optical depths $\tau \ll 1$) play a potentially important role in the earth's atmosphere. However, their tenuous nature makes them difficult to detect, and as a result there are few quantitative, global analyses of them. The Moderate Resolution Imaging Spectrometer (MODIS) on board the *Terra* satellite has a channel at 1.375 μm that is specifically designed to detect these clouds, and can measure optical depths as low as 0.02 with an uncertainty factor of 2. During two 3-day periods from December 2000 and June 2001, about one-third of the pixels flagged as cloud free by the MODIS cloud mask are shown to contain detectible thin cirrus. These thin cirrus generally have optical depths below ~0.05 and appear with greater frequency and optical depth near deep convection.

1. Introduction

A casual glance at the sky reveals that clouds exist in many shapes and sizes. Previous research has shown that these clouds play a crucial role in determining the radiative, meteorological, and chemical state of the atmosphere. One type in particular, cirrus clouds, has been identified as one of the most uncertain components in atmospheric research, as evidenced by the volume of research (e.g., Liou 1986; Stephens et al. 1990; Minnis et al. 1993; Mishchenko et al. 1996; Baum et al. 2000) and number of field campaigns [e.g., the First International Satellite Cloud Climatology Project (ISCCP) Regional Experiment (FIRE; Starr 1987), Subsonic Aircraft: Contrail and Cloud Effects Special Study (SUCCESS; Toon and Miake-Lye 1998), and the Cirrus Regional Study of Tropical Anvils and Cirrus Layers-Florida Area Cirrus Experiment (CRYSTAL-FACE)] dedicated to their study.

While the effects of cirrus clouds are dominated by optically thick ones, thin cirrus clouds (optical depth $\tau \ll 1$ in the visible and near infrared), especially those in the tropical upper troposphere, have emerged as potentially important for two reasons. First, they are potentially radiatively important (e.g., McFarquhar et al. 2000; Jensen et al. 1996; Hartmann et al. 2001; Prabhakara et al. 1993). Second, they potentially play an important role in the dehydration of air entering the stratosphere (e.g., Jensen et al. 2001; Holton and Gettelman 2001).

A primary hindrance to evaluating the importance of these thin cirrus is the difficulty in measuring them, which arises primarily due to their low optical depth. Prabharkara et al. (1993) use measured radiances in the midinfrared from nadir-viewing satellite-borne instruments to derive optical depths of thin clouds (Prabhakara et al. 1993, their Fig. 4). However, their measurements had a detection limit of ~0.25, so these data only marginally qualify as thin cirrus. Satellite-borne limb-viewing instruments such as the Stratospheric and Aerosol Gas Experiment (SAGE) and Cryogenic Limb Array Etalon Spectrometer (CLAES) observe the clouds from the side and can therefore see optical depths as low as 10^{-6} (Wang et al. 1996; Mergenthaler et al. 1999). The principal disadvantage of these data is that their measurements are averaged over horizontal length scales of hundreds of km and vertical length scales of a few km, making these measurements somewhat difficult to interpret. And for all previous satellite datasets, limitations of the data required averaging over months in order to develop a global view. Active methods, such as lidars, can detect thin clouds with unprecedented resolution (Winker and Trepte 1998; Nee et al. 1998; McFarquhar et al. 2000; Sassen and Cho 1992), but these data are presently limited in both time and space.

In this paper, we use data from the Moderate Resolution Imaging Spectrometer (MODIS; King et al. 1992)

Corresponding author address: Dr. Andrew Dessler, ESSIC/University of Maryland at College Park, 2207 Computer and Space Science Bldg., College Park, MD 20742.
E-mail: dessler@atmos.umd.edu

on board the National Aeronautics and Space Administration's (NASA's) *Terra* spacecraft to study the spatial distribution and occurrence frequency of thin cirrus in the Tropics during two 3-day periods. These MODIS data represent an improvement in our ability to measure thin cirrus. First, MODIS is a nadir-viewing imaging spectrometer that samples with the high horizontal resolution (1 km $\times$ 1 km). Second, it contains a channel at 1.375 μm that was specifically designed to measure thin cirrus optical depths $\ll$0.1. As a result, MODIS is capable of providing a global view with both high sensitivity and high horizontal resolution.

TABLE 1. Electronic cross-talk adjustment coefficients (%). Detector number is in "product order." The adjustment is the percent of band-5 radiance subtracted from band-26 radiance to adjust for cross talk and is relevant for data taken during the period between Nov 2000 and Jun 2001 when *Terra* MODIS was running on the "b-side" electronics. Coefficients from C. Moeller (2002, personal communication).

Detector no.	Adjustment	Detector no.	Adjustment
1	1.9	6	1.4
2	1.5	7	1.4
3	1.2	8	1.6
4	1.2	9	2.0
5	1.2	10	2.9

2. Data and methodology

a. Terra MODIS data

Terra is in a sun-synchronous, 705-km orbit, with its descending orbit crossing the equator at 1030 local time (LT). Two time periods are considered in this analysis: 6–8 December 2000 and 6–8 June 2001. In this paper, we will use the 1-km resolution calibrated radiances (MOD02) and the 1-km cloud mask and cirrus reflectance products from the cloud product (MOD06). All data are version 3.

The primary data used in this paper are the radiances at 1.375 μm ($r_{1.375}$), which is entirely reflected solar radiation. Because of strong water vapor absorption at this wavelength, little upwelling radiance from low clouds or the surface reaches the satellite. Upwelling radiance from cirrus clouds, which are located above $\sim$10-km altitude and above $\sim$99% of the atmospheric water vapor, experiences relatively little attenuation. Furthermore, this wavelength is sufficiently long that Rayleigh scattering from the atmosphere is negligible. As a result, this wavelength is sensitive to clouds in the upper troposphere or lower stratosphere (Gao et al. 1993).

There are known data quality issues associated with the *Terra* MODIS 1.375-μm radiance data that must be considered before the data are applied to our analysis. The first is a light leak into the detector at $\sim$5.2 μm, which contaminates the 1.375-μm band. This leak is small and appears to be corrected in processing of the data prior to distribution. The second is electronic cross talk between bands on the short and mid-wavelength infrared focal plane (1.24–4.5 μm), which includes the 1.375-μm detector.

The magnitude of the cross talk was determined by researchers at the Cooperative Institute for Meteorological Satellite Studies (CIMSS), University of Wisconsin (C. Moeller 2002, personal communication). They regressed 1.375-μm radiances against band-5 (1.240 μm) radiances for clear-sky daytime scenes over land. Band 5 was selected to represent the contamination because of its close spectral proximity to a spectral leak in the 1.375-μm filter observed in prelaunch testing. For these scenes, the real signal at 1.375 μm should be approximately zero, so it was assumed that any signal in the channel originated from cross talk. The slope of the regression, which was done on a detector-by-detector basis, is the fraction of band-5 radiance that is leaking into the 1.375-μm band (listed in Table 1). By subtracting this fraction of 1.240-μm radiance from the 1.375-μm, we can correct for the cross talk. There is no evidence that these coefficients varied during the 6-month period considered in this paper. All of the data used in this paper have been adjusted in this way.

b. Calculation of optical depth

For the very small optical depths considered here ($\tau \ll 1$), photons originating from single-scattering events dominate the total radiance (Yang et al. 2001). In this case, we can relate cirrus reflectivity r_c at 1.375 μm to the 1.375-μm optical depth τ through the following relation:

$$\tau = r_c \frac{4 \cos\theta_s \cos\theta_v}{P(\Theta)\tilde{\omega}}, \qquad (1)$$

where θ_s and θ_v are the solar and satellite zenith angles, respectively. Here $P(\Theta)$ is the phase function and Θ is the scattering angle (a function of θ_s and θ_v and ϕ, the relative azimuth angle between the sun and satellite). We use phase function calculations described by Yang et al. (2001); these calculations assume a size distribution with a mean maximum dimension of 20.6 μm and an effective size of 8.9 μm for a mixture of crystal habits including hexagonal plates, hollow columns, bullet rosettes, and aggregates. The detailed description of the phase function calculation can be found in Baum et al. (2000). Here $\tilde{\omega}$ is the single-scattering albedo. Because ice does not absorb strongly in the near-infrared, we assume $\tilde{\omega}$ is 1.

The satellite does not directly measure cirrus reflectivity r_c, but instead measures the reflectivity at the top of the atmosphere, $r_{1.375}$. This latter quantity is smaller than r_c because absorption by water vapor above the cirrus cloud reduces the reflected radiance from upper-tropospheric thin cirrus by as much as a few tens of percent. Gao et al. (1998; Gao et al. 2002, manuscript submitted to *IEEE Trans. Geosci. Remote Sens.*) have developed a method to remove this absorption through an empirical scene-by-scene regression between these data and radiances from a wavelength (0.66 μm over land and 1.24 μm over ocean) that water does not absorb. The algorithm has been implemented in the MODIS level-2 operational production and this cirrus reflectivity is stored in the MOD06 level-2 product.

Ideally, we would have simply used them in Eq. (1). However, they have not been corrected for electronic cross talk. So instead, we use in Eq. (1) the cross talk–corrected $r_{1.375}$ increased by the ratio of cirrus reflectivity in the MOD06 granule to the uncorrected $r_{1.375}$ in the MOD02 granule. This correction increases radiance on average about 30%. Further, we throw out any data whose water vapor correction increases $r_{1.375}$ by more than 50%. This insures that the reflecting cloud is in the upper troposphere. Finally, we include in this analysis only those pixels for which the satellite zenith angle is less than 45° to avoid complications associated with the three-dimensional effect of clouds and the spherical atmosphere.

1) Limitations of the method

Reflected radiance from low- and midlevel clouds at 1.375 μm is greatly attenuated by water vapor absorption, but such absorption is not necessarily complete (e.g., Fig. 4 of Gao and Kaufman 1995). And in dry regions of the atmosphere, such as over deserts, reflection from the surface can reach the satellite. Because the reflectance from thin cirrus is so small ($r_c \ll 1\%$), a small signal from the surface or low clouds could swamp the signal from thin cirrus. To avoid this, we restrict our analysis to cloud-free pixels over water.

To determine which pixels are cloud free, we use the 99% probability–clear threshold of the MODIS cloud mask product (Ackerman et al. 1998). The version of the cloud mask used in this paper, version 3, flags pixels as cloudy if their optical depths are 0.2–0.3 (S. Ackerman 2002, personal communication). The surface type is determined using the U. S. Geological Survey global land/water mask, which is stored with the cloud mask.

2) Uncertainty in the retrieved optical depth

Uncertainty in the derived optical depth arises from errors in the measured $r_{1.375}$, errors in the conversion from $r_{1.375}$ to r_c, and errors in the conversion from r_c to optical depth τ.

Because the signal at 1.375 μm at the ground is small, determining the accuracy of these measurements is difficult. However, comparisons between the MODIS measurements of other reflected solar bands, which water does not absorb, and at-satellite radiance predicted by ground-based measurements combined with radiative transfer calculations are good (Thome et al. 2002, unpublished manuscript). By analogy, it is expected that the calibration of the 1.375-μm radiances is similarly good and it is estimated that the accuracy of these data is 30% (K. Thome 2002, personal communication). Because we are analyzing clear-sky pixels over water exclusively, where the signal in band 5 (1.240 μm) is minimized, electronic cross talk between band 5 and the 1.375-μm band is expected to be a minor contributor to the total uncertainty (although an adjustment is made for it anyway). We estimate that the adjustment for upper-tropospheric water vapor, that is, the calculation of r_c from $r_{1.375}$, introduces a ~20% uncertainty.

Virtually all of the uncertainty in the conversion of reflectivity to optical depth [Eq. (1)] is contained in the phase function. While the uncertainty in this is difficult to quantify, we can get an idea of its magnitude by using a phase function that corresponds to a much larger size distribution (effective size of 78 μm). Using this phase function increases the calculated average τ by a factor of 1.4. We assume based on this that the uncertainty in the conversion from reflectivity to optical depth is ~40%. Combining these various uncertainties, we conclude that the accuracy of the derived optical depth is a factor of 2.

We can estimate the precision of the reflectivity measurement using nighttime data, when the signal at 1.375 μm and the other reflected solar bands should be zero. Based on this, we estimate the precision of an individual measurement of $r_{1.375}$ to be twice the standard deviation of nighttime data, $2\sigma \approx 5 \times 10^{-4}$. For typical conditions, this means that the precision uncertainty of the optical depth τ is ~0.01. To be conservative, we will assume that any measurement of $\tau > 0.02$ in an individual pixel cannot be explained by uncertainty and represents an upper-tropospheric thin cirrus cloud.

3) Comparison with lidar data

To validate our retrieval, we compare optical depths determined from the MODIS with those measured by a micropulse lidar at the Nauru Island Atmospheric Radiation Measurement (ARM) site (0.521°S, 166.916°E; Campbell et al. 2002). Every other day, *Terra* MODIS makes thin cirrus optical depth measurements over the Nauru site around 1030 LT. For each overpass between 1 April and 24 May 2001, the optical depth measurements made within 10 km of the Nauru site are averaged to yield a single MODIS-derived value of thin cirrus optical depth.

For the lidar, backscatter profiles are averaged over 2 min and an optical depth is calculated from the average profile (Comstock and Sassen 2001). Five 2-min averages are then averaged to create a single 10-min average centered around the overpass time. The uncertainty of the lidar-derived optical depth is ±24%, due primarily to uncertainty in the backscatter-to-extinction ratio. lidar-derived cirrus optical depths over Nauru have been compared with radar results (Comstock et al. 2002), which reveal good correlation between the independent

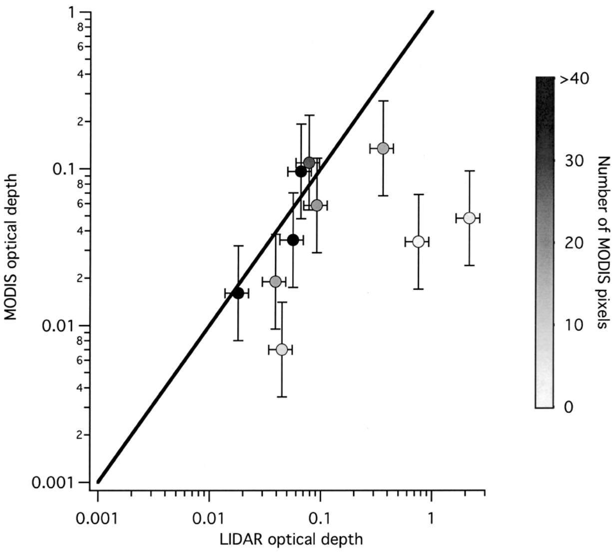

FIG. 1. Comparison between MODIS and Nauru micropulse lidar optical depths made between 1 Apr and 24 May 2001. Lidar optical depths are a 10-min average around the satellite overpass time; MODIS optical depths are averages of all measurements (cloud free over water) within 10 km of the lidar site. Shading of the points indicates the number of MODIS pixels that went into the average. Error bars are ±24% for lidar and a factor of 2 for MODIS.

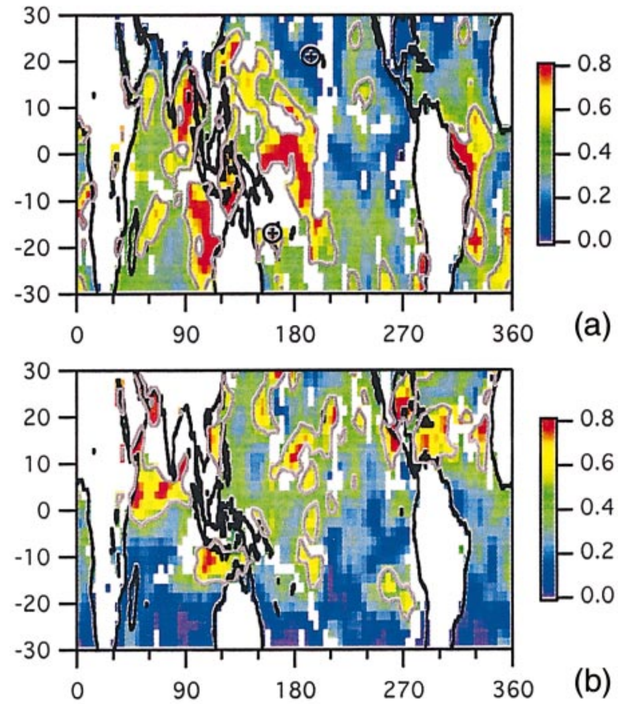

FIG. 2. Fraction of observations (color scale) between latitudes 30°N and 30°S and longitudes 0° to 360° during the (a) 6–8 Dec 2000 and (b) 6–8 Jun 2001 time periods whose optical depth τ exceeded 0.02. White indicates less than 1000 measurements in the box. The + symbols in (a) are the locations from which the histograms in Figs. 3b and 3c are derived. The fields have been smoothed to emphasize the large-scale structure. Gray contours indicate the 30% frequency contour for $\tau > 0.03$.

ground-based measurements. Finally, we consider here only lidar optical depth calculations for clouds above 9 km, which can only be made in the absence of low-level clouds.

Figure 1 shows the comparison between the MODIS and lidar optical depths. The points are shaded according to how many of the MODIS pixels around the lidar site were categorized as cloud free by the cloud mask and were therefore included in the average. Dark points indicate overpasses when the sky around Nauru was generally free of thick clouds. In these cases, which are expected to provide the best comparison, the agreement between the MODIS and the lidar is good.

As the occurrence of thick clouds in the region increases (and the shading of the points becomes lighter), the lidar measures systematically higher optical depths than the MODIS. This occurs because the MODIS only calculates optical depth in pixels that are flagged as cloud free ($\tau <$ 0.2–0.3), while the lidar measurement uses no such threshold. As a result, in cloudy regions, the lidar is expected to be higher than the MODIS, and that is indeed what is observed. Based on Fig. 1, we conclude that the thin cirrus optical depth retrieved by MODIS is accurate to within the stated uncertainty.

3. Thin cirrus frequency and average optical depth

To construct the figures in this section, we obtained daytime MODIS granules data between 30°N and 30°S for the two 3-day periods being analyzed. To determine the thin cirrus frequency, pixel-level measurements of τ are segregated into boxes 4° of longitude by 2° of latitude. In Fig. 2, we plot the fraction of measurements in each box whose $\tau > 0.02$. It is important to remember that only pixels over water and flagged as cloud free by the MODIS cloud mask are included, and that the cloud mask flags clouds with optical depths of 0.2–0.3.

The plot of the frequency of $\tau > 0.03$ is qualitatively similar, but with the frequency about 20% lower. As an example, the gray contours in Fig. 2 indicate the region where 30% of the pixels have $\tau > 0.03$. It should be noted that a visible optical depth of 0.03 is the generally accepted definition for ‘‘subvisible cirrus’’ (Sassen and Cho 1992), and that visible and 1.375-μm optical depths are expected to differ by only a few percent.

Figure 3a shows a histogram of the $>10^7$ individual measurements of optical depth from 6–8 December 2000. Note that the distribution is strongly peaked at low optical depths—62% of the observations have $\tau <$ 0.02, 90% have $\tau < 0.05$, and 97% have $\tau < 0.1$. Using $\tau = 0.02$ as the detection limit, about 38% and 28% of the pixels observed during the 6–8 December 2000 and 6–8 June 2001 periods, respectively, have some detectible thin cirrus in them.

Figure 2a has two symbols (circumscribed plus signs).

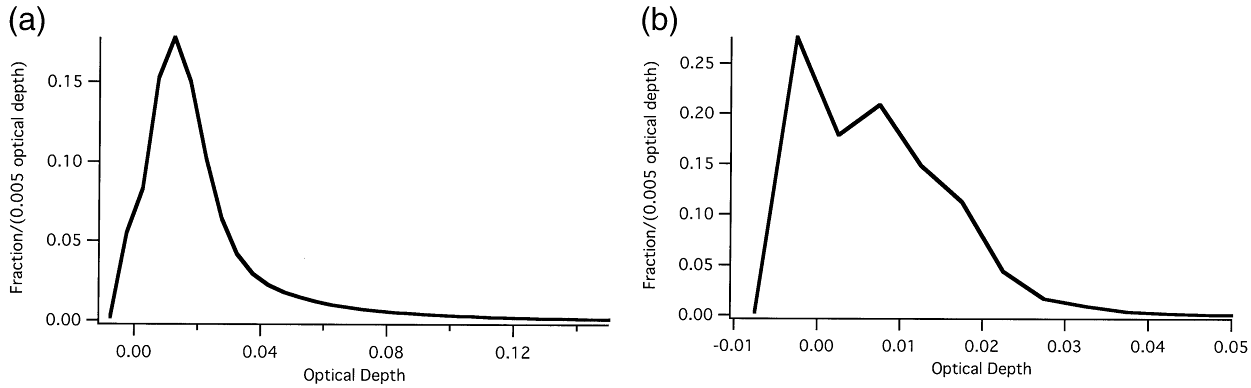

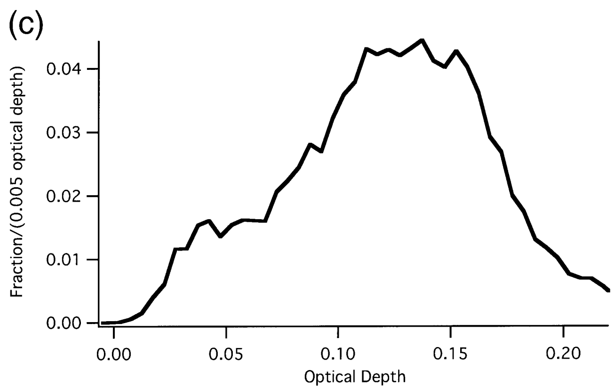

FIG. 3. Histograms of optical depth (τ) from the 6–8 Dec 2000 time period; (a) all of the pixels in Fig. 2a. (b) All of the pixels from the box centered at 21°N, 166°W, in a region of low occurrence of thin cirrus. (c) All of the pixels from the box centered at 17°S, 162°E, in a region of high occurrence. Note that the x and y axes of these three plots are different.

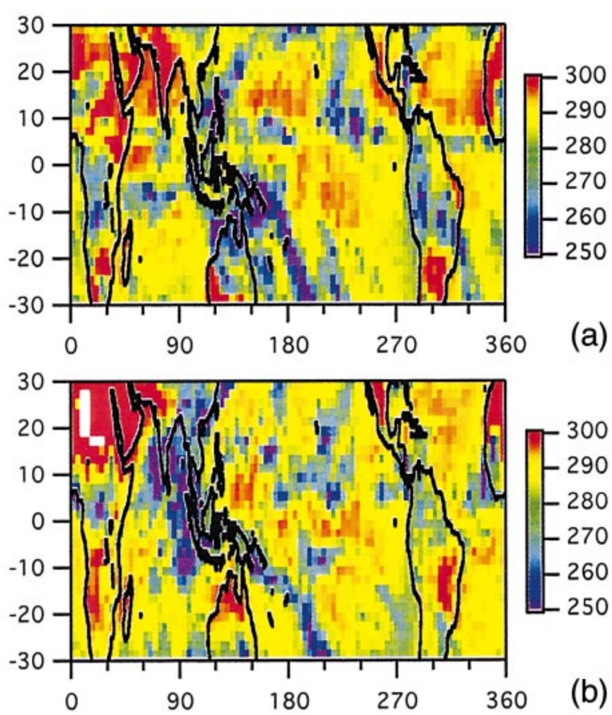

FIG. 4. Average 11-μm brightness temperature (K, color shading) between latitudes 30°N and 30°S and longitudes 0° to 360° for the (a) 6–8 Dec 2000 and (b) 6–8 Jun 2001 time periods. The average is calculated for all pixels (clear and cloudy) over both land and ocean.

One is near Hawaii and is located in a region of low occurrence of thin cirrus. The other is east of Australia and is in a region of high occurrence. A histogram of the region near Hawaii is plotted in Fig. 3b. The average τ in this box is 0.007—92% of the pixels in this region have $\tau < 0.02$—below the detection limit and therefore indistinguishable in our dataset from clear sky, although more sensitive methods may detect very thin clouds in this region. Also note that the histogram shows that some of the pixels have negative optical depths. This is a result of the precision uncertainty in the individual pixels, which leads to some negative values of r_c.

A histogram of the region east of Australia is plotted in Fig. 3c, a region of high occurrence of thin cirrus. This plot shows frequencies for an optical depth peak between 0.10 and 0.15, with a rapid falloff for higher and lower optical depths. The falloff on the high end could represent a real decrease in the occurrence of pixels with larger optical depths, or it can result from the cloud mask flagging these pixels as ‘‘cloudy’’ with increasing probability. The average τ in this box is 0.12. Only 0.6% of the pixels in this region have optical depth $\tau < 0.02$, below the detection limit, while 92% have $\tau > 0.05$. In other words, virtually every pixel in this region has some cloud in it.

Figure 4 shows the average 11-μm brightness temperature (T_{11}) for the two periods. This was obtained by binning and averaging all of the T_{11} measurements in each latitude–longitude box, including those flagged as

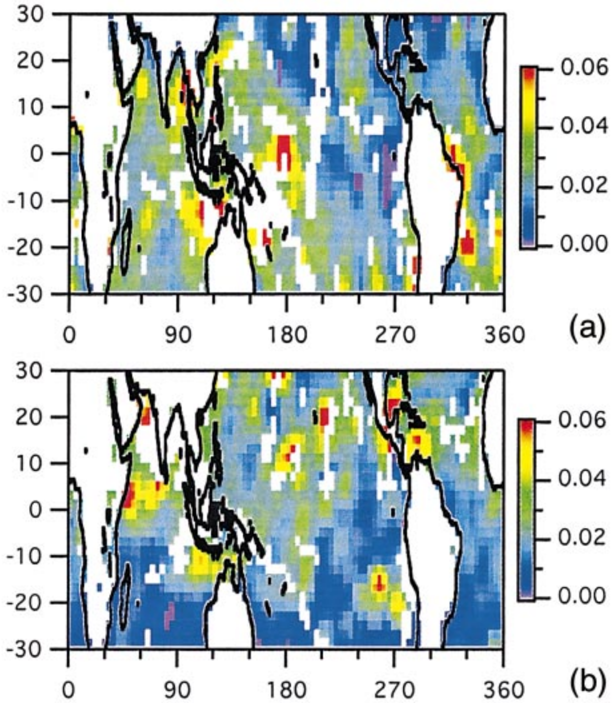

FIG. 5. Average optical depth τ (color shading) between latitudes 30°N and 30°S and longitudes 0° to 360° for the (a) 6–8 Dec 2000 and (b) 6–8 Jun 2001 time periods. White indicates less than 1000 measurements in the box. The fields have been smoothed to emphasize the large-scale structure.

cloudy or over land. The colder temperatures indicate high, thick clouds, which are the result of deep convection. Warmer temperatures indicate the region is free of deep convection.

Figures 2 and 4 show that thin cirrus occurs more frequently near deep convection. In other words, regions of high occurrence frequency, such as east of Australia in December, tend to be close to deep convection. Regions of low occurrence frequency, such as near Hawaii, are not. This observation is consistent with the most likely theories of thin cirrus formation, either as blow-off from convective systems or cooling from uplift associated with synoptic and mesoscale systems (Pfister et al. 2001; Massie et al. 2002).

Importantly, our analysis is the first one to look at this correlation on time periods as short as a few days. Previous work (Wang et al. 1996; Mergenthaler et al. 1999; Prabhakara et al. 1988) has shown that this correlation holds when averaged over months, and ours shows that it holds on timescales of a few days.

The average τ in each $4° \times 2°$ box is plotted in Fig. 5. Note that because of the large number of points going into each box, the standard error of the average is negligible. In this case, the detection limit is significantly smaller than the single-pixel threshold of 0.02; we estimate it to be $\sim$0.002 based on the precision of the nighttime data. The accuracy estimate of a factor of 2 is unchanged by averaging. The tropical average optical depth τ was 0.023 and 0.018 in the December and June time periods, respectively. This figure tells a story similar to Fig. 2. High values of average optical depth are located near deep convection, again suggesting that convection is the source of these thin clouds.

One of the intriguing aspects of these data is the high value of frequency and average optical depth off the west coast of North Africa in June (Fig. 5b). It is well known that large quantities of dust blow off the continent and over the ocean in this location. If this dust gets lofted to high altitudes, then it is possible that this signal is not due to cirrus clouds but due to dust. More research on this is necessary before anything more definite can be said.

4. Discussion and conclusions

In this paper, we describe a method for retrieving thin cirrus optical depth at 1.375 μm using data from the *Terra* MODIS instrument. These data represent a step forward in our ability to quantitatively identify thin cirrus clouds.

Due to instrument and algorithm limitations, thin cirrus optical depth τ can only be retrieved in pixels that are over water and have been flagged as ''clear sky'' by the MODIS cloud mask, which flags clouds with optical depths greater than about 0.2–0.3 in the current version of the software. The necessity to retrieve over clear-sky means that we cannot comment on whether the thin cirrus overlap other clouds, in particular deep convection. The uncertainty in the retrieved optical depth is estimated to be a factor of 2.

During two 3-day periods, we find that these thin cirrus clouds are ubiquitous in the Tropics, but tend to occur more frequently near deep convection. Taking the Tropics as a whole, the vast majority of thin cirrus clouds have $\tau < 0.05$. Overall, about one-third of the individual pixels contained detectible thin cirrus. It is almost certain that a more sensitive method or instrument would see a higher fraction of clouds.

The limited time period covered in this paper was imposed by the enormous amount of data that the MODIS produces—one day of MODIS 1-km calibrated radiance occupies 67 gigabytes of disk space. Doing analyses over weeks, months, or years will require enhancements in the data distribution infrastructure. Such enhancements are likely to occur in the near future and we hope to revisit this problem at that time. Another limitation is that the satellite's morning equator crossing time and the requirement of sunlight provides us with a morning view of thin cirrus only. When data from the recently launched *Aqua* satellite become available, an afternoon view of thin cirrus will become available.

The work has not proved or disproved whether thin cirrus are important, but it has bolstered the idea that they are ubiquitous. Therefore, an important role for them cannot be ruled out and they must continue to be carefully considered in future analyses of the upper troposphere.

Acknowledgments. This work was supported by the NASA New Investigator Program in Earth Science and a NASA EOS/IDS grant to the University of Maryland. Chris Moeller helped greatly with the band-26 correction algorithms. Jennifer Comstock graciously did the Nauru lidar intercomparison. Steve Ackerman, Bob Ellingson, Steve Platnick, Steve Sherwood, and Kurt Thome provided useful comments. We would especially like to thank Steve Kempler and the rest of the crew at the Goddard Space Flight Center Earth Sciences Data and Information Services Center Distributed Active Archive Center for their hard work in getting us the MODIS data.

REFERENCES

Ackerman, S. A., K. I. Strabala, W. P. Menzel, R. A. Frey, C. C. Moeller, and L. E. Gumley, 1998: Discriminating clear sky from clouds with MODIS. *J. Geophys. Res.,* **103,** 32 141–32 157.

Baum, B. A., D. P. Kratz, P. Yang, S. C. Ou, Y. X. Hu, P. F. Soulen, and S. C. Tsay, 2000: Remote sensing of cloud properties using MODIS airborne simulator imagery during SUCCESS. Part 1. Data and models. *J. Geophys. Res.,* **105,** 11 767–11 780.

Campbell, J. R., D. L. Hlavka, E. J. Welton, C. J. Flynn, D. D. Turner, J. D. Spinhirne, V. S. Scott, and I. H. Hwang, 2002: Full-time, eye-safe cloud and aerosol lidar observation at atmospheric radiation measurement program sites: Instruments and data processing. *J. Atmos. Oceanic Technol.,* **19,** 431–442.

Comstock, J. M., and K. Sassen, 2001: Retrieval of cirrus cloud radiative and backscattering properties using combined lidar and infrared radiometer (LIRAD) measurements. *J. Atmos. Oceanic Technol.,* **18,** 1658–1673.

——, T. P. Ackerman, and G. G. Mace, 2002: Ground based lidar and radar remote sensing of tropical cirrus clouds at Nauru Island: Cloud statistics and radiative impacts. *J. Geophys. Res.,* in press.

Gao, B.-C., and Y. J. Kaufman, 1995: Selection of the 1.375-μm MODIS channel for remote sensing of cirrus clouds and stratospheric aerosols from space. *J. Atmos. Sci.,* **52,** 4231–4237.

——, A. F. H. Goetz, and W. J. Wiscombe, 1993: Cirrus cloud detection from airborne imaging spectrometer data using the 1.38 μm water vapor band. *Geophys. Res. Lett.,* **20,** 301–304.

——, Y. J. Kaufman, W. Han, and W. J. Wiscombe, 1998: Correction of thin cirrus path radiances in the 0.4–1.0 μm spectral region using the sensitive 1.375 μm cirrus detecting channel. *J. Geophys. Res.,* **103,** 32 169–32 176.

Gao, B.-C., P. Yang, W. Han, R. R. Li, and W. J. Wiscombe, 2002: An algorithm using visible and 1.38 μm channels to retrieve cirrus reflectances from aircraft and satellite data. *IEEE Trans. Geosci. Remote Sens.,* **40,** 1659–1668.

Hartmann, D. L., J. R. Holton, and Q. Fu, 2001: The heat balance of the tropical tropopause, cirrus, and stratospheric dehydration. *Geophys. Res. Lett.,* **28,** 1969–1972.

Holton, J. R., and A. Gettelman, 2001: Horizontal transport and the dehydration of the stratosphere. *Geophys. Res. Lett.,* **28,** 2799–2802.

Jensen, E. J., O. B. Toon, H. B. Selkirk, J. D. Spinhirne, and M. R. Schoeberl, 1996: On the formation and persistence of subvisible cirrus clouds near the tropical tropopause. *J. Geophys. Res.,* **101,** 21 361–21 375.

——, L. Pfister, A. S. Ackerman, A. Tabazadeh, and O. B. Toon, 2001: A conceptual model of the dehydration of air due to freeze-drying by optically thin, laminar cirrus rising slowly across the tropical tropopause. *J. Geophys. Res.,* **106,** 17 237–17 252.

King, M. D., Y. J. Kaufman, W. P. Menzel, and D. Tanre, 1992: Remote-sensing of cloud, aerosol, and water-vapor properties from the Moderate Resolution Imaging Spectrometer (MODIS). *IEEE Trans. Geosci. Remote Sens.,* **30,** 2–27.

Liou, K. N., 1986: Influence of cirrus clouds on weather and climate processes: A global perspective. *Mon. Wea. Rev.,* **114,** 1167–1199.

Massie, S., A. Gettelman, W. Randel, and D. Baumgardner, 2002: The distribution of tropical cirrus in relation to convection. *J. Geophys. Res.,* in press.

McFarquhar, G. M., A. J. Heymsfield, J. Spinhirne, and B. Hart, 2000: Thin and subvisual tropopause tropical cirrus: Observations and radiative impacts. *J. Atmos. Sci.,* **57,** 1841–1853.

Mergenthaler, J. L., A. E. Roche, J. B. Kumer, and G. A. Ely, 1999: Cryogenic Limb Array Etalon Spectrometer observations of tropical cirrus. *J. Geophys. Res.,* **104,** 22 183–22 194.

Minnis, P., K. N. Liou, and Y. Takano, 1993: Inference of cirrus cloud properties using satellite-observed visible and infrared radiances. Part II: Verification of theoretical cirrus radiative properties. *J. Atmos. Sci.,* **50,** 1305–1322.

Mishchenko, M. I., W. B. Rossow, A. Macke, and A. A. Lacis, 1996: Sensitivity of cirrus cloud albedo, bidirectional reflectance and optical thickness retrieval accuracy to ice particle shape. *J. Geophys. Res.,* **101,** 16 973–16 985.

Nee, J. B., C. N. Len, W. N. Chen, and C. I. Lin, 1998: Lidar observation of the cirrus cloud in the tropopause at Chung-Li (25°N, 121°E). *J. Atmos. Sci.,* **55,** 2249–2257.

Pfister, L., and Coauthors, 2001: Aircraft observations of thin cirrus clouds near the tropical tropopause. *J. Geophys. Res.,* **106,** 9765–9786.

Prabhakara, C., R. S. Fraser, G. Dalu, M. L. C. Wu, R. J. Curran, and T. Styles, 1988: Thin cirrus clouds: Seasonal distribution over oceans deduced from *Nimbus-4* IRIS. *J. Appl. Meteor.,* **27,** 379–399.

——, D. P. Kratz, J.-M. Yoo, G. Dalu, and A. Vernekar, 1993: Optically thin cirrus clouds: Radiative impact on the warm pool. *J. Quant. Spectrosc. Radiat. Transfer,* **49,** 467–483.

Sassen, K., and B. S. Cho, 1992: Subvisual thin cirrus lidar dataset for satellite verification and climatological research. *J. Appl. Meteor.,* **31,** 1275–1285.

Starr, D. O'C. 1987: A cirrus-cloud experiment: Intensive field observations planned for FIRE. *Bull. Amer. Meteor. Soc.,* **68,** 119–124.

Stephens, G. L., S. C. Tsay, P. W. Stackhouse, and P. J. Flatau, 1990: The relevance of the microphysical and radiative properties of cirrus clouds to climate and climate feedback. *J. Atmos. Sci.,* **47,** 1742–1753.

Toon, O. B., and R. C. Miake-Lye, 1998: Subsonic aircraft: Contrail and cloud effects special study (SUCCESS). *Geophys. Res. Lett.,* **25,** 1109–1112.

Wang, P. H., P. Minnis, M. P. McCormick, G. S. Kent, and K. M. Skeens, 1996: A 6-year climatology of cloud occurrence frequency from Stratospheric Aerosol and Gas Experiment II observations (1985–1990). *J. Geophys. Res.,* **101,** 29 407–29 429.

Winker, D. M., and C. R. Trepte, 1998: Laminar cirrus observed near the tropical tropopause by LITE. *Geophys. Res. Lett.,* **25,** 3351–3354.

Yang, P., and Coauthors, 2001: Sensitivity of cirrus bidirectional reflectance to vertical inhomogeneity of ice crystal habits and size distributions for two MODIS bands. *J. Geophys. Res.,* **106,** 17 267–17 291.